# Intracellular Processing of Poly(Ethylene Imine)/Ribozyme Complexes Can Be Observed in Living Cells by Using Confocal Laser Scanning Microscopy and Inhibitor Experiments

**Thomas Merdan,[1,2] Klaus Kunath,[1] Dagmar Fischer,[1] Jindrich Kopecek,[2] and Thomas Kissel[1,3]**

*Received October 17, 2001; accepted November 7, 2001*

***Purpose.*** Critical steps in the subcellular processing of poly(ethylene imine)/nucleic acid complexes, especially endosomal/lysosomal escape, were visualized by using living cell confocal laser scanning microscopy (CSLM) to obtain an insight into their mechanism.

***Methods.*** Living cell confocal microscopy was used to examine the intracellular fate of poly(ethylene imine)/ribozyme and poly(L-lysine)/ribozyme complexes over time, in the presence of and without bafilomycin A1, a selective inhibitor of endosomal/lysosomal acidification. The compartment of complex accumulation was identified by confocal microscopy with a fluorescent acidotropic dye. To confirm microscopic data, luciferase reporter gene expression was determined under similar experimental conditions.

***Results.*** Poly(ethylene imine)/ribozyme complexes accumulate in acidic vesicles, most probably lysosomes. Release of complexes occurs in a sudden event, very likely due to bursting of these organelles. After release, poly(ethylene imine) and ribozyme spread throughout the cell, during which slight differences in distribution between cytosol and nucleus are visible. No lysosomal escape was observed with poly(L-lysine)/ribozyme complexes or when poly(ethylene imine)/ribozyme complexes were applied together with bafilomycin A1. Poly(ethylene imine)/plasmid complexes exhibited a high luciferase expression, which was reduced approximately 200-fold when lysosomal acidification was suppressed with bafilomycin A1.

***Conclusions.*** Our data provide, for the first time, direct experimental evidence for the escape of poly(ethylene imine)/nucleic acid complexes from the endosomal/lysosomal compartment. CLSM, in conjunction with living cell microscopy, is a promising tool for studying the subcellular fate of polyplexes in nucleic acid/gene delivery.

**KEY WORDS:** polyethylenimine; intracellular processing; living cell confocal microscopy; lysosomal escape.

## INTRODUCTION

Poly(ethylene imine) (PEI) is one of the most commonly used nonviral vectors based on polycations for DNA/RNA delivery both *in vitro* and *in vivo* (1). Despite numerous publications dealing with the mechanisms of uptake and subcellular processing of PEI/plasmid complexes, current understanding of the release mechanism from the endosomal/lysosomal compartment is still limited (1–3). New insights could facilitate the design of new polymers for nonviral gene delivery systems. It has been shown by several groups that PEI is taken up via endocytosis (4,5); however, theories for uptake and intracellular processing of PEI polyplexes remain controversial. Using confocal microscopy studies, Godbey *et al* (3) found that PEI/plasmid complexes access cells in culture via endocytosis. According to Godbey *et al* (2), these endocytotic vesicles do not seem to fuse with lysosomes but, rather, proceed directly to the perinuclear region where PEI and DNA are released and taken up into the nucleus (2,3). Furthermore, Lecocq *et al* (4) examined uptake and subcellular distribution of radioactively labeled PEI *in vivo* by using differential and isopycnic centrifugation methods. They observed that PEI was localised in plasma membrane fractions 5 min after administration and in lysosomal fractions after 4 h. According to this study, PEI persists in the lysosomal compartment without significant release for days. Another unclear, yet very important question, is how PEI/nucleic acid complexes escape from the endosomal/lysosomal compartment. Behr (6,7) proposed the so-called "proton-sponge hypothesis" explaining the lysosomal release of PEI polyplexes by their buffering capacity. During acidification of endosomes/lysosomes, this property leads to increased influx of protons, chloride ions, and water, thus eventually causing rupture of the vesicles due to the high osmotic pressure. Although this hypothesis was developed some years ago, no experimental verification has been provided so far.

Ribozymes have attracted particular attention, because of their unique ability to cleave and deactivate messenger RNA in a sequence-specific manner, enabling a selective down- regulation of gene expression. Approaches using ribozymes are under development against a variety of targets, including multidrug resistance (MDR1) in cancer chemotherapy (8) or HER-2 overexpression (9), as well as antiviral ribozymes against *e.g.,* HIV, CMV, *etc.* (10). From a drug delivery perspective, ribozymes are very attractive, because they are smaller in size than plasmids and do not require delivery into the nucleus to exert biological activity.

Recently, we studied PEI as delivery vehicle for ribozymes, because it is not only an efficient agent for intracellular delivery but also stabilizes ribozymes against enzymatic degradation (unpublished data). Many intriguing questions as to the mechanism of PEI/ribozyme subcellular trafficking remain unanswered.

In this report we attempt to gain insight into these subcellular distribution processes of PEI/ribozyme complexes by using living cell confocal laser scanning microscopy. This method is unique, because it allows a direct observation of PEI/nucleic acid complexes in the intact subcellular environment over a long time. More specifically, it may prove to be a valuable tool in elucidating the release mechanism of PEI polyplexes from the endosomal/lysosomal compartment.

PEI/ribozyme complexes were used in the presence of and without bafilomycin A1, a selective inhibitor of the vacuolar-type H(+)-ATPase, which prevents acidification of endosomes/lysosomes. Our aim was to gain a mechanistic insight in subcellular processing of dually labeled PEI/ribozyme complexes by observing fluorescence distribution over time.

[1] Department of Pharmaceutics and Biopharmacy, Philipps University, Ketzerbach 63, 35032, Marburg, Germany.

[2] Department of Pharmaceutics and Pharmaceutical Chemistry, The University of Utah, 30 South, 2000 East, Salt Lake City, Utah.

[3] To whom correspondence should be addressed. (e-mail: kissel@mailer.uni-marburg.de)

0724-8741/02/0200-0140/0 

## MATERIALS AND METHODS

### Chemicals

Poly(ethylene imine) (MW 25,000), poly(L-lysine) (MW 34,300), chloroquine, and bafilomycin A1 were purchased from Sigma-Aldrich.

### Labeling of PEI and Poly(L-Lysine) with Oregon Green 488

Polymer (20 mg) was dissolved in 2 mL 0.1 M sodium bicarbonate solution pH 9. Oregon Green carboxylic acid succinimidyl ester (1 mg; Molecular Probes) was dissolved in 200 μL dimethylsulfoxide and added dropwise under stirring to the polymer solution. The mixture was stirred in the dark for 3 h at room temperature before the labeled polymer was purified by ultrafiltration in an Amicon cell (regenerated cellulose membrane, MW cutoff 10,000) and washed with 0.1 M borate/1.0 M sodium chloride solution, pH 7.5. The washing procedure was performed until no absorption was detectable at 488 nm in the cell outflow. As a final step, the buffer was exchanged with distilled water.

### Ribozyme and Plasmid

A 5-carboxytetramethylrhodamine labeled 37-mer ribozyme with the sequence 3′-UCUCUCAAAGCAGGAUUGCCUGAGUAGUCAUAACCUU-5′ was purchased from MWG-Biotech. A luciferase plasmid (pGL3-control; Promega) was used for transfection experiments. The plasmid was amplified in JM109 competent cells (Promega) and purified with QIAfilter plasmid Kits (Qiagen) according to the manufacturer's protocol.

### Complex Formation

All ribozyme/PEI or plasmid/PEI complexes were prepared at a PEI-nitrogen to DNA/RNA-phosphate ratio (N/P ratio) of 8. For microscopic experiments, ribozyme (2 μg) and PEI (2.2 μg) were each dissolved in 100 μL of 0.9 % sodium chloride solution pH 7. The two solutions were mixed by gentle pipetting. Complexes were allowed to interact for 10 min before use. Ribozyme/poly(L-lysine) and plasmid/poly(L-lysine) complexes were prepared at an N/P ratio of 2. In this case, 2 μg of ribozyme and 1.6 μg poly(L-lysine) were dissolved in 100 μL 0.9 % sodium chloride solution, pH 7. For transfection experiments using pGL3-control luciferase plasmid, complexes were prepared in a similar manner with 4 μg plasmid and 4.4 μg PEI or 3.2 μg poly(L-lysine) dissolved in double the volume of sodium chloride solution 0.9%, pH 7.

### Cell Culture

All experiments were performed with the SW13 adrenal gland carcinoma cell line (ATCC number CCL-105), which was a kind gift from Dr. A. Aigner (Philipps University, Marburg, Germany). Cells were cultured in IMDM medium (PAA) containing glutamine (584 mg/L) and 25 mM 4-(2-hydroxyethyl)-1-piperazine ethane sulfonic acid (HEPES), supplemented with 10% fetal bovine serum (HyClone). For transfection experiments, cells were grown at 37°C in a humidified atmosphere containing 10% $CO_2$ (v/v).

### Confocal Laser Scanning Microscopy with Lyso Tracker Blue

A Zeiss Axiovert 100 M microscope coupled to a Zeiss LSM 510 scanning device was used for all confocal microscopy experiments.

Cells were seeded at a density of 20,000 cells per well in eight-well chamber slides (LabTek, Nunc). After 24 h, medium was removed and complexes of Oregon Green-labeled PEI and nonlabeled pGL3-control plasmid were added in new medium containing 100 nM Lyso Tracker Blue (Molecular Probes). After 1 h the incubation medium was aspirated, cells were washed three times with phosphate buffered saline (PBS) pH 7, and observed in PBS with the confocal microscope. For excitation of the blue Lyso Tracker, an Enterprise UV laser with an excitation wavelength of 364 nm was used. For excitation of green fluorescence (labeled PEI), an argon laser with an excitation wavelength of 488 nm was used. This experiment was performed by using a long-pass filter of 385 nm for blue fluorescence and a long-pass filter of 505 nm for green fluorescence. All images were recorded by using the Zeiss LSM 510 Multitracking Mode in which each fluorescence channel was scanned individually.

### Living Cell Confocal Laser Scanning Microscopy

An argon laser was used to excite green fluorescence at 488 nm and a helium-neon laser was used for red fluorescence at 543 nm. Images were taken by using a band-pass filter of 505–530 nm for green fluorescence and a long-pass filter of 560 nm for red fluorescence. Detector sensitivity was set relatively high to be able to visualize faint fluorescence and was kept constant during experiments. Thickness of the optical sections was between 0.5 and 1 μm. Stacks of 15–35 images were recorded every 3–9 min to obtain information over time (setting descriptions for the individual figure are listed below each figure). The different layers were overlaid for each time point by Zeiss LSM 510 software. For creating movies the overlaid images of the single time points were animated over time. Total thickness of stacks ranged between 10 and 20 μm. Temperature was maintained at 37°C for the duration of the experiment. A $CO_2$ atmosphere was not necessary, because the cell culture medium contained 25 mM HEPES. For living cell microscopy, 30,000 cells were seeded on 2-$cm^2$ self-made chamber dishes containing a total of 500 μL of medium. Bafilomycin A1 was added to the media at a concentration of 300 nM, where indicated.

### Transfection Experiments with Luciferase Plasmid

Transfection experiments with pGL3-control luciferase plasmid were performed with poly(L-lysine)/plasmid complexes in addition to PEI/plasmid complexes in the presence of, as well as without bafilomycin A1. Cells were seeded in 12-well plates at a density of 50,000 cells per well. After 24 h medium was removed and complexes were added to fresh medium containing 300 nM bafilomycin A1, when applicable. Media were exchanged again after 4 h, and cells were incubated for 44 h. Luciferase gene expression was quantified by using a commercial kit (Promega) and photon counting with a luminometer (Sirius, Berthold).

Results in relative light units per second (RLU/s) were converted into ng luciferase by creating a calibration curve

with recombinant luciferase (Promega). Protein concentration in each sample was determined by using a BCA assay (11). All experiments were performed in quintuplet, and data were expressed in ng luciferase per mg protein.

## RESULTS

### Confocal Laser Scanning Microscopy Using Lyso Tracker Blue

In Fig. 1, colocalization of PEI/DNA complexes (green) and Lyso Tracker Blue is shown ~1 h after transfection (turquoise vesicles). Several predominantly green vesicles are also present in this image. These could either represent PEI in nonacidic prelysosomal compartments or in lysosome remnants, suggesting that in this case the lysosomes had already burst. This strongly indicates that complexes accumulate in the lysosomal compartment after 1 h. We obtained similar results with OVCAR-3 (ATCC number HTB-161) cells (data not shown).

### Living Cell Confocal Laser Scanning Microscopy

Five short movies have been chosen to show the results of living cell confocal laser scanning microscopy (see Table I). Movies 1 and 2 were obtained with PEI/ribozyme complexes. Movie 3 shows PEI/ribozyme complexes in the presence of 300 nM bafilomycin A1, and Movie 4 was recorded by using poly(L-lysine)/ribozyme complexes. Movie 5 shows an overview of ~20 cells incubated with PEI/ribozyme complexes, whereas only the green fluorescence of PEI is shown. All movies can be accessed as supplementary material for this publication on our web site http://www.uni-marburg.de/iptb/institut/akkissel/motherpage.htm. Essential excerpts from Movies 1 and 2 are shown in Figs. 2 and 3. It should be noted that the vesicle sizes in Movies 1–5 do not accurately display actual sizes, because of fluorescence outshine; however, relative changes in localization and size over time can be observed.

In Figs. 2 and 3 (Movies 1 and 2) it is shown that PEI/ribozyme complexes and also some free PEI, resulting from an N/P ratio of 8, adhere to the cellular membrane within a few minutes after incubation, possibly because of interactions between positively charged complexes and the negative charges of certain membrane constituents. Time of uptake into cells is rather heterogeneous. In several cells, uptake is very rapid, occurring ~10–15 min after incubation (*e.g.,* Fig. 3, Movie 2). In other cells, internalization seems to be much slower (*e.g.,* several cells shown in Fig. 2, Movie 1).

Under the conditions used in this experiment (*i.e.,* microscope settings), some PEI-containing vesicles display a very typical appearance (Fig. 2, Image 1, vesicle marked with yellow arrow; Fig. 3, Images 1–7). The inner core of these vesicles is yellow, indicating that ribozyme and PEI are colocalized here, whereas a very small surrounding "corona" is green, which implies that PEI is predominantly located in this area. This "corona" might represent interactions between PEI and components of the lysosomal membrane and/or extensive swelling of the polymer matrix in proximity to the vesicular membrane. Separation of PEI and ribozyme close to the membrane might be another possible explanation for this appearance.

The size of the vesicle in Fig. 2, Image 1 (marked with the yellow arrow) seems to increase within the 9 min between Images 1 and 3, possibly because of osmotic swelling or fusion with other PEI-containing vesicles. Finally, it releases its content into the cytoplasm (Fig. 2a, Image 4). After this event, the whole cell, including the nuclear compartment, is filled with a faint green-yellow fluorescence, resulting from the mixture of green fluorescence from PEI (predominantly) and the red fluorescence from ribozyme (very faint). This fluorescence can be seen only with sensitive instrument settings but is significantly brighter than background fluorescence. If distribution of fluorescence in the different confocal layers is regarded before and after endosomal/lysosomal burst, one finds a significant increase of fluorescence throughout the whole cell after burst. In Fig. 2b it can be seen that the distribution of fluorescence is not totally homogeneous after burst. These images represent the fluorescence in a single confocal layer of 1-μm thickness before and after burst. The area exhibiting slightly less intense fluorescence may likely display the nuclear compartment. However, it should be noted that both green and red fluorescence also increase significantly in this area, thus implying that PEI and ribozyme are present in the nucleus a maximum of 3 min after burst. The complete sectioning of the whole cell can be accessed on our supplementary material web site. The remnant of the burst vesicle is predominantly red and seems to consist of ribozyme and PEI, whereas relatively more ribozyme seems to be present than before burst. It persists in the cytosol and only changes its size and color marginally. The further fate of these remnants is unclear and requires a more thorough investigation. In most of the cells only a small percentage of vesicles burst. Most of the PEI/ribozyme complexes persists

**Table I.** Characteristics of Movies Accessible on Our Web Site

| Movie | Type of experiments | Excerpts in figure | Colors |
|---|---|---|---|
| 1 | PEI/ribozyme complexes | Figure 2 | PEI green, ribozyme red |
| 2 | PEI/ribozyme complexes | Figure 3 | PEI green, ribozyme red |
| 3 | PEI/ribozyme complexes with bafilomycin A1 | | PEI green, ribozyme red |
| 4 | Poly(L-lysine)/ribozyme complexes | | Poly(L-lysine) green, ribozyme red |
| 5 | PEI/ribozyme complexes overview | | PEI green |

In addition, the complete sections of Images 3 and 4 from Fig. 2 can be regarded. The web site is optimized for Microsoft Internet Explorer and a resolution of 1024 × 768 pixels.

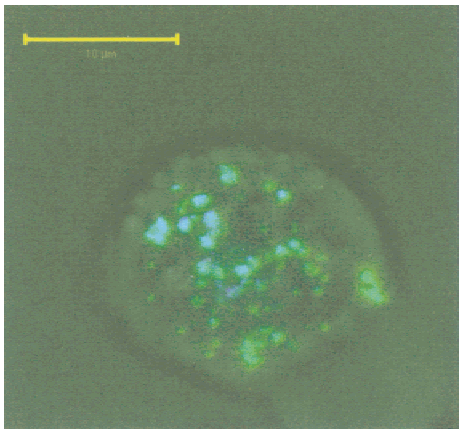

**Fig. 1.** PEI/plasmid complexes colocalize with Lyso Tracker Blue ~1 h after incubation (turquoise vesicles). In addition, vesicles containing predominantly PEI are visible (green vesicles). The image shows an overlay of light microscopic and confocal fluorescence image. (Lyso Tracker is blue in this image; PEI is green).

in the endosomal/lysosomal compartment for a minimum of several hours or longer (4).

In Fig. 3 (Movie 2) three cells that contain enormous amounts of PEI/ribozyme complexes can be seen. Although under average conditions vesicle burst occurs only once or twice per cell, this example is suitable to show the mechanism of escape. In this case, a clear sequential increase in fluorescence in the cells after burst of individual vesicles can be readily observed. Vesicles move in a random fashion within the cells and also fuse to create larger vesicles (in Fig. 3 Images 1–4). Between Images 3 and 4 some vesicles seem to burst (arrow in Image 3), thus initiating a disastrous process for these cells. Within the next ~20 min, a chain reaction takes place during which all vesicles in these three cells burst and release their contents into the cytosol (yellow arrows in images of Fig. 3 mark vesicles that have burst in the next image). A possible explanation for this phenomenon could be the destabilizing effect of PEI on the lysosomal membrane not only from the inner compartment but from the cytosolic side, as well (5). Once one lysosome releases its content, PEI is present in the cytosol and can destabilize other vesicles that are still intact. The more endosomes/lysosomes that rupture, the more PEI is released and the higher is the destabilizing potential present in the cytosol. This process may progress until all vesicles have burst, as shown in this example. The distribution of fluorescence throughout cells after destabilization of vesicles can be observed very well in this sequence. It is of interest that there seems to be an accumulation of green and red fluorescence in the nucleus of cell number 2 in Fig. 3. This accumulation might display interactions of the high PEI and ribozyme concentrations present in this cell with DNA in the nucleus.

It is important to note that the timescale for uptake and lysosomal release of the PEI/ribozyme complexes is very heterogeneous, occurring after 20 min in some cells, whereas in others the process may take hours for unknown reasons.

Movie 5 on our supplementary material web site shows

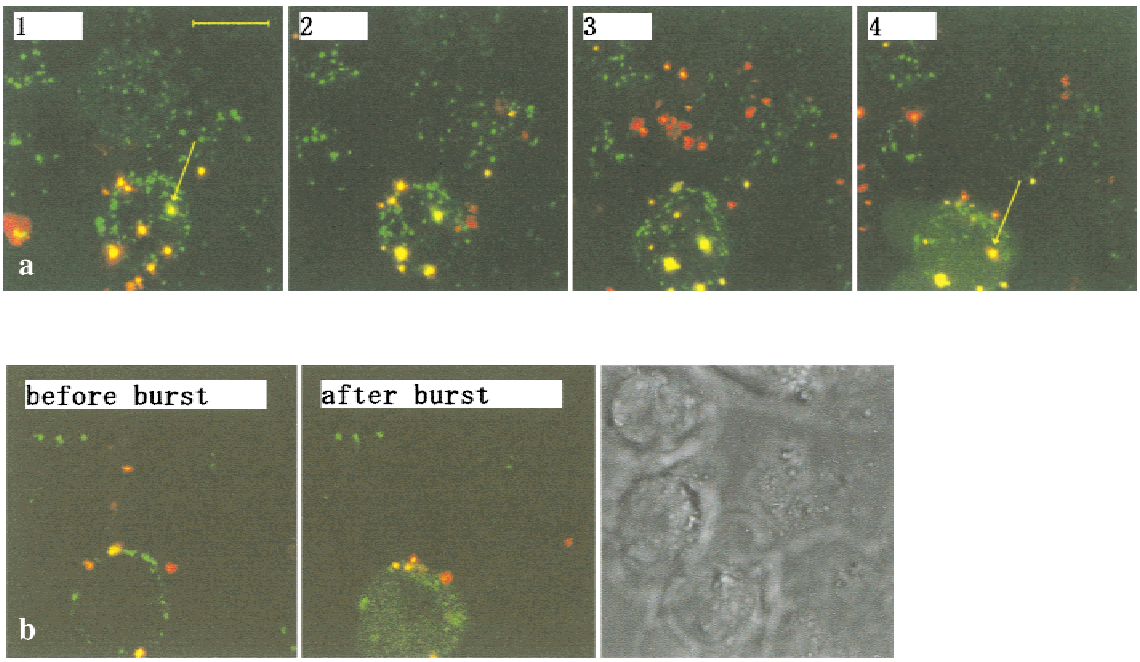


**Fig. 2.** (a) Living cell microscopic visualization of swelling and, finally, bursting of a single vesicle (yellow arrow). PEI is green and ribozyme is red in this sequence. Before burst, the characteristic appearance of the vesicle with a yellow core and green PEI-corona can be seen. Afterward, the faint green-yellow fluorescence can be seen evenly distributed throughout the entire cell. The remnant of the vesicle is significantly smaller and deeper red. Images were recorded 28, 31, 37, and 40 min after incubation. They display computer-overlaid projections of the different confocal slices for each time point. The whole movie can be accessed on our web site (Movie 1). The yellow mark displays the size of 10 μm. (b) The same confocal layer of 1 μm thickness before and after lysosomal burst (37 and 40 min after incubation). It may be observed that fluorescence intensity increases throughout the whole cell after burst, whereas there seems to be an area where it is slightly weaker. This area might display the nucleus. The right image shows a light microscopic image. The complete sectioning of this cell for the 37- and 40-min time point can be accessed on our web site.

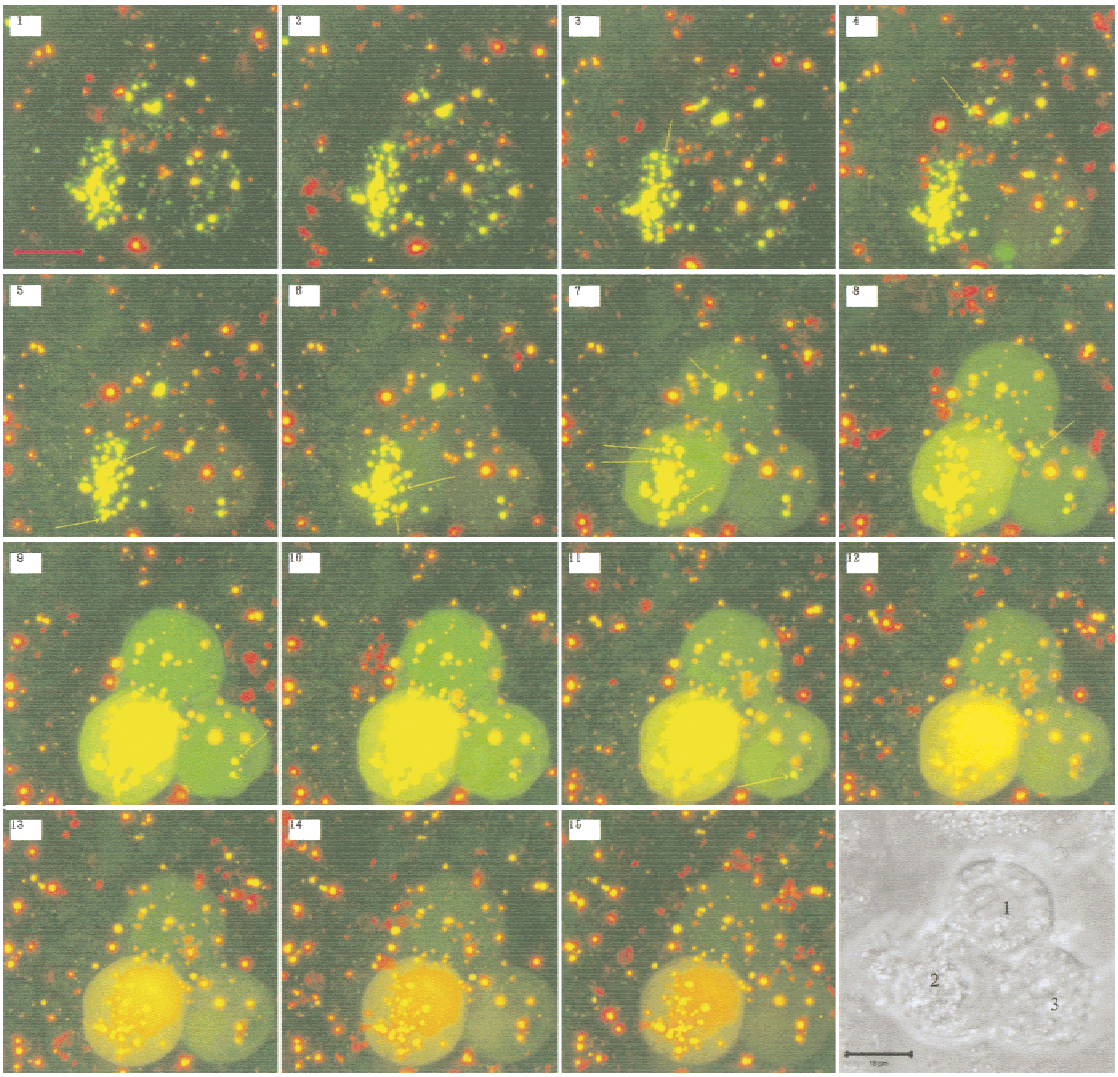


**Fig. 3.** Living cell microscopic images of three cells loaded with enormous amounts of PEI/ribozyme complexes. PEI is green and ribozyme is red in this sequence. Vesicles start bursting between Images 3 and 4. In the next ~20 min, all vesicles release their content. Yellow arrows point out vesicles that have already burst in the next image. For example, Image 8 shows the evenly distributed fluorescence throughout cells 1 and 3. In cell 2, obvious interactions between PEI and ribozyme with nuclear constituents occur, and in this case a fluorescence remains in the nucleus. Images were recorded every 3 min starting 15 min after incubation. Images 1–15 are duo fluorescence images derived from the computer-aided overlay of different confocal layers for each time point. Image 16 is a light microscopy image to show positions and numbers of the cells. The whole movie can be accessed on our web site (Movie 2).

an overview of ~20 cells, thus showing that data shown here is representative. In this movie the bursting of several endosomes/lysosomes can be observed as a sudden increase of green fluorescence (PEI) within cells indicated by yellow arrows. In addition, the sequential increase in fluorescence within one particular cell can be observed.

When the acidification of lysosomes was prevented by using 300 nM bafilomycin A1, no bursting of lysosomes could be observed over a period of 4 h (data shown in Movie 3 on our supplementary material web site). Cells examined under these conditions take up complexes as efficiently as without bafilomycin A1. The vesicles move within the cells in a disorganized manner; however, no escape of PEI or ribozyme can be observed.

Using poly(L-lysine)/ribozyme complexes under similar experimental conditions showed that complexes were taken up into cells efficiently; however, there was no bursting of lysosomes or other visible escape route from this compartment (Movie 4 on our Internet pages).

### Transfection Experiments with Luciferase Plasmid

Transfection experiments with PEI/luciferase-plasmid complexes at N/P = 8 led to a high reporter gene expression (Fig. 4). In the presence of bafilomycin A1, however, expression was decreased >200-fold. This finding stresses the great importance of endosomal/lysosomal acidification for the release of complexes from this compartment. With poly(L-lysine)/plasmid complexes only a very low transfection efficiency could be observed, suggesting that these complexes are not as readily able to leave endosomes/lysosomes. These data are in good agreement with our microscopic observations.

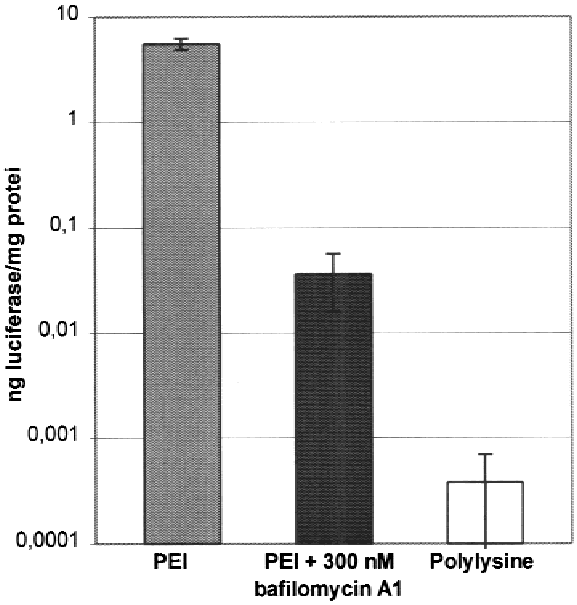


**Fig. 4.** Luciferase reporter gene expression of PEI in the presence of and without bafilomycin A1 and using polylysine.

## DISCUSSION

The subcellular trafficking of PEI/ribozyme complexes could be observed by using living cell confocal microscopy. Especially the escape from the endosomal/lysosomal compartment, as well as the distribution of PEI and RNA after this event could be visualized for the first time. We also showed that acidification is equally essential for the release of PEI/RNA polyplexes, as for efficient gene expression after application of PEI/luciferase-plasmid complexes.

Complexes of PEI and DNA/RNA reach the lysosomal compartment. This may be concluded from our microscopic data with the acidotropic Lyso Tracker, which is in agreement with the results of subcellular fractionation experiments using PEI *in vivo* (4). In contrast, Godbey *et al* (2) found PEI located in nonacidic structures by using confocal laser scanning microscopy. A possible explanation for this discrepancy could be that, in this case, nonintact endosomes or lysosomes were observed. Instead, remnants of lysosomes, such as those in the last images of Figs. 2 and 3 could have been observed. These compartments are no longer acidic and, therefore, do not accumulate acidotropic agents, such as Lyso Tracker Blue.

Concerning the escape mechanism of PEI/RNA complexes from endosomes/lysosomes, our results show that release occurs as a sudden event, such as the bursting or rupture of endosomes or lysosomes. No release of PEI-polyplexes from endosomes/lysosomes was observed, however, when acidification of these vesicles was prevented. In addition, there was a dramatic reduction of luciferase reporter gene expression in the presence of bafilomycin A1, a finding that is consistent with recent results of Kichler *et al* (12). The manifest importance of endosomal/lysosomal acidification suggests that the buffering capacity of PEI is one of the crucial properties of the polymer for its high efficiency in DNA/RNA delivery. There is evidence in the literature that this is one of the key features that cationic polymers require to obtain high transfection efficiencies. Cationic polymers with strong basic groups (*e.g.,* poly(L-lysine) or quaternary amines with poor to no buffering properties possess low-transfection efficiencies when used without chloroquine (13–15) or other lysosome-destabilizing agents (16). In contrast, polymers with a significant buffering capacity in the lysosomal pH range show a much higher transfection capability. For example, imidazole-containing polymers (17–19) exhibit a high reporter gene expression, very likely due to the pKa of imidazole (~6). Midoux and Monsigny (20) performed transfection experiments in the presence of bafilomycin A1 and, similar to our results, reporter gene expression was reduced >100-fold compared to experiments without inhibition of endosomal/lysosomal acidification. Other examples of polymers supporting these findings include polyamidoamine dendrimers (21,22) or fractured dendrimers (23). These groups of polymers are quite similar to PEI because they also exhibit a large number of terminal amino groups on their surface and higher-order amines in their interior, whereas not all amino groups are protonated at physiologic pH. Transfection efficiencies with these polymers are significantly higher than those obtained, *e.g.,* with poly(L-lysine), and it is likely that efficient endosomal/lysosomal release is at least part of the reason for this. Further examples in literature of effective nucleic acid delivery agents with titratable groups between pH 5 and 7 include lipospermines (24) and poly[2-(N,N-dimethylamino)ethyl methacrylate] (25), which both exhibit good transfection efficiencies.

These similar findings with structurally unrelated agents suggest that several requirements must be fulfilled for an efficient transfection with cationic polymers. The polymer must be of low toxicity and, because of its three-dimensional structure, capable to effectively complex with DNA/RNA at physiologic pH. It also needs to possess a certain buffering capacity between pH 5 and 7. These factors enable effective uptake and a sufficient release from the endosomal/lysosomal compartment, thus leading to the desired gene expression or ribozyme action.

As suggested by Behr (6), the buffering capacity of the polymer could lead to lysosomal swelling based on two possible mechanisms: an increased $H^+/Cl^-$/water influx and possible swelling of the polymer network as a result of the increasing electrostatic repulsion of charged groups. Both effects eventually lead to rupture of vesicles and release of their contents into the cytosol. In our study it is remarkable that PEI and ribozyme are distributed throughout the cytoplasm and nucleus minutes after endosomal/lysosomal burst, because of the fact that PEI/ribozyme complexes are rather stable. The cause of this could be the extension of the polymer network during acidification or interactions of PEI with the lysosomal membrane or cytoplasm constituents. Both effects could lead to destabilization of the complexes and enhanced dissociation after release from vesicles. Interactions of cationic lipoplexes and negatively charged lipids have been previously shown (26). In addition, other pH-dependent interactions of polyplexes with the endosomal/lysosomal membrane could play an important role for efficient escape from vesicles.

A very important question that remains to be answered is: At what stage of the endosomal/lysosomal pathway does bursting of the vesicles occur? Although our data and the findings of Lecocq *et al* (4) suggest that most polymer accumulates in lysosomes, release could also occur from late endosomes. If release takes place from lysosomes, the simultaneous release of lysosomal content, such as hydrolytic enzymes, might be harmful for cells (27). This could be one

mechanism of toxicity of PEI/nucleic acid complexes and might be a limiting factor for this branch of nonviral nucleic acid delivery.

Another intensively discussed point is the mode of entry of PEI and DNA/RNA into the nucleus. Our results indicate that no cell division is necessary for the entry of PEI and ribozyme, a finding that has also been shown for plasmids by Pollard *et al* (7). The entry of PEI and ribozyme into the nucleus in our experiments could occur via diffusion, as implied by the high speed of the process. This is a reasonable assumption, based on the fact that ribozyme and PEI have molecular weights of ~11 and ~25 kD, respectively, and therefore, could be small enough to diffuse through the nuclear pore complex. The maximum size for this form of nuclear entry has been determined as ~50 kD (28). PEI could promote this process by compacting the ribozyme in such a way as to facilitate nuclear entry. In addition, negatively charged phospholipids might coat these structures, such as suggested by Godbey *et al* (3) to allow for an easier nuclear entry. This mechanism, however, is speculative and requires a more detailed investigation. For plasmids, on the other hand, the free diffusion or coating mechanism is unlikely, because of their large size. In this case, a condensation caused by PEI may also play a crucial role, although the nuclear transfer is much more inefficient (7). Interactions between plasmid or plasmid/PEI and the nuclear pore complex might be considered. Experiments investigating the nuclear entry of plasmids are in progress at this time.

In summary, CSLM in living cells allows visualization of subcellular trafficking of PEI/RNA complexes and sheds some light on the mechanism, as well as kinetics of their endosomal/lysosomal escape. Our data are compatible with the "proton sponge hypothesis" (6); however, other pH-dependent membrane interactions of the polycation may play a significant role for the escape of polyplexes into the cytoplasm as well. CSLM in living cells may be a valuable tool for the design of more efficient nonviral vectors based on polycations in gene delivery.

## REFERENCES


1. W. T. Godbey, K. K. Wu, and A. G. Mikos. Poly(ethylenimine) and its role in gene delivery. *J. Control. Release* **60**:149–160 (1999).
2. W. T. Godbey, M. A. Barry, P. Saggau, K. K. Wu, and A. G. Mikos. Poly(ethylenimine)-mediated transfection: a new paradigm for gene delivery. *J. Biomed. Mater. Res.* **51**:321–328 (2000).
3. W. T. Godbey, K. K. Wu, and A. G. Mikos. Tracking the intracellular path of poly(ethylenimine)/DNA complexes for gene delivery. *Proc. Natl. Acad. Sci. USA* **96**:5177–5181 (1999).
4. M. Lecocq, S. Wattiaux-De Conink, N. Laurent, R. Wattiaux, and M. Jadot. Uptake and intracellular fate of polyethylenimine *in vivo*. *Biochem Biophys. Res. Commun.* **278**:414–418 (2000).
5. A. R. Klemm, D. Young, and J. B. Lloyd. Effects of polyethyleneimine on endocytosis and lysosome stability. *Biochem. Pharmacol.* **56**:41–46 (1998).
6. J. P. Behr. The proton sponge—a trick to enter cells the viruses did not exploit. *Chimia* **51:**34–36 (1997).
7. H. Pollard, J .S. Remy, G. Loussouarn, S. Demolombe, J. P. Behr, and D. Escande. Polyethyleneimine, but not cationic lipids promotes transgene delivery to the nucleus in mammalian cells. *J. Biol. Chem.* **273**:7507–7511 (1998).
8. Y. Masuda, H. Kobayashi, J. F. Holland, and T. Ohnuma. Reversal of multidrug resistance by a liposome-MDR1 ribozyme complex. *Cancer Chemother. Pharmacol.* **42**:9–16 (1998).
9. A. Aigner, S. S. Hsieh, C. Malerczyk, and F. Czubayko. Reversal of HER-2 over- expression renders human ovarian cancer cells highly resistant to taxol. *Toxicology* **144**:221–228 (2000).
10. K. Konopka, J. J. Rossi, P. Swiderski, V. A. Slepushkin, and N. Duzgunes. Delivery of an anti-HIV-1 ribozyme into HIV-infected cells via cationic liposomes. *Biochim. Biophys. Acta* **1372**:55–68 (1998).
11. H. D. Hill and J. G. Straka. Protein determination using bicinchoninic acid in the presence of sulfhydryl reagents. *Anal. Biochem.* **170**:203–208 (1988).
12. A. Kichler, C. Leborgne, E. Coeytaux, and O. Danos. Polyethylenimine-mediated genedelivery: a mechanistic study. *J Gene Med.* **3**:135–144 (2001).
13. P. Erbacher, A. C. Roche, M. Monsigny, and P. Midoux. Putative role of chloroquine in gene transfer into a human hepatoma cell line by DNA/lactosylated polylysine complexes. *Exp. Cell. Res.* **225**:186–194 (1996).
14. M. A. Wolfert, P. R. Dash, O. Nazarova, D. Oupicky, L. W. Seymour, S. Smart, J. Strohalm, and K. Ulbrich. Polyelectrolyte vectors for gene delivery: influence of cationic polymer on biophysical properties of complexes formed with DNA. *Bioconjug. Chem.* **10**:993–1004 (1999).
15. M. A. Wolfert, E. H. Schacht, V. Toncheva, K. Ulbrich, O. Nazarova, and L. W. Seymour. Characterization of vectors for gene therapy formed by self-assembly of DNA with synthetic block co-polymers. *Hum. Gene Ther.* **7**:2123–2133 (1996).
16. E. Wagner, C. Plank, K. Zatloukal, M. Cotton, and M. L. Birnstiel. Influenza virus hemagglutinin HA-2 N-terminal fusogenic peptides augment gene transfer by transferrin-polylysine-DNA complexes: toward a synthetic virus-like gene-transfer vehicle. *Proc. Natl. Acad. Sci. USA* **89**:7934–7938 (1992).
17. C. Pichon, M. B. Roufai, M. Monsigny, and P. Midoux. Histidylated oligolysines increase the transmembrane passage and the biological activity of antisense oligonucleotides. *Nucleic Acids Res.* **28**:504–512 (2000).
18. D. Putnam, C. A. Gentry, D. W. Pack, and R. Langer. Polymer-based gene delivery with low cytotoxicity by a unique balance of side-chain termini. *Proc. Natl. Acad. Sci. USA* **98**:1200–1205 (2001).
19. D. W. Pack, D. Putnam, and R. Langer. Design of imidazole-containing endosomolytic biopolymers for gene delivery. *Biotechnol. Bioeng.* **67**:217–223 (2000).
20. P. Midoux and M. Monsigny. Efficient gene transfer by histidylated polylysine/pDNA complexes. *Bioconjug. Chem.* **10**:406–411 (1999).
21. J. Haensler and F. C. Szoka. Polyamidoamine cascade polymers mediate efficient transfection of cells in culture. *Bioconjug. Chem.* **5**:372–379 (1993).
22. Z. Y. Zhang and B. D. Smith. High-generation polycationic dendrimers are unusually effective at disrupting anionic vesicles: membrane bending model. *Bioconjug. Chem.* **11**:805–814 (2000).
23. M. X. Tang, C. T. Redemann, and F. C. Szoka Jr. In vitro gene delivery by degraded polyamidoamine dendrimers. *Bioconjug. Chem.* **7**:703–714 (1996).
24. B. Sola, C. Staedel, J. S. Remy, A. Bahr, and J. P. Behr. Lipospermine-mediated gene transfer technique into murine cultured cortical cells. *J. Neurosci. Methods* **71**:183–186 (1997).
25. P. van de Wetering, E. E. Moret, N. M. Schuurmans-Nieuwenbroek, M. J. van Steenbergen, and W. E. Hennink. Structure-activity relationships of water-soluble cationic methacrylate/methacrylamide polymers for nonviral gene delivery. *Bioconjug. Chem.* **10**:589–597 (1999).
26. Y. Xu and F. Szoka Jr. Mechanism of DNA release from cationic liposome/DNA complexes used in cell transfection. *Biochemistry* **35**:5616–5623 (1996).
27. U. T. Brunk, H. Dalen, K. Roberg, and H. B. Hellquist. Photo-oxidative disruption of lysosomal membranes causes apoptosis of cultured human fibroblasts. *Free Radic. Biol. Med.* **23**:616–626 (1997).
28. B. Talcott and M. S. Moore. Getting across the nuclear pore complex. *Trends Cell Biol.* **9**:312–318 (1999)